Numerical simulations of the 8 September 1905 Calabrian tsunami (southern Italy) as a tool to improve the assessment of tsunami risk on the Calabrian coast

Stefano Tinti and Alessio Piatanesi

Department of Physics, University of Bologna, Bologna, Italy[1]

Abstract. This paper presents a study of the tsunami following the disastrous earthquake that hit Calabria, southern Italy on 8 September 1905. According to contemporary sources the tsunami caused damage and flooded low lands in several segments of the coast. Our analysis is carried out by means of numerical modeling and aims at giving a contribution to the assessment of the seismic and tsunami risk in this region. The source fault of the earthquake is still controversial. We simulate three tsunamis produced by sources that can be proposed basing on macroseismic data analysis and on the present seismotectonic knowledge of the region, namely the Capo Vaticano (CV) fault, the Vibo Valentia (VV) fault, and the Lamezia (LA) fault. We compute water waves assuming that the sea bottom displacement is caused by shear dislocation over a rectangular fault according to Okada's formulas, and use the shallow water approximation to study wave propagation. The result of our study is that we cannot distinguish between CV and VV sources: both respect some historical observations, while failing to fulfill others. Possibly the agreement can be improved by suitable tuning of the parameters of the fault mechanism. On the other hand, we are able to conclude that fault LA is very unlikely to be the tsunami source, since it is found to produce a perturbation that is too weak. A further interesting result is that only a small fraction of tsunami energy penetrates the Messina strait to the south.

1. Introduction

During the last centuries the largest tsunamigenic earthquakes that hit the Italian peninsula occurred in Calabria and Sicily, the two Italian regions most exposed to earthquake and tsunami risk. In previous papers we studied some of these events: e.g., the 1693 eastern Sicily (Piatanesi and Tinti, 1998; Tinti *et al.*, 2001), the 1783 southern Calabria (Tinti and Piatanesi, 1996) and the 1908 Messina Strait (Piatanesi *et al.*, 1999; Tinti *et al.*, 1999) earthquakes, all reaching the maximum intensity XI of the Mercalli-Cancani-Sieberg (MCS) scale. The tsunami considered in this work was caused by an earthquake shaking southern Calabria on 8 September 1905 at around 01:43 a.m. local time. Almost total destruction was caused to several towns on the Tyrrhenian side of Calabria, from Capo Suvero to Capo Vaticano (see Fig. 1). Some damage was also reported in the Aeolian Islands and in numerous villages of the province of Messina in Sicily. Casualties exceeded 550, over 2000 people were injured and about 300,000 remained homeless. The tsunami was observed in the open sea and along the coast, and its effects were succinctly described by several coeval authors (e.g., Baratta, 1906; Platania, 1907; see also the catalogue of the Italian tsunamis by Tinti and Maramai, 1996). In the epicentral area several segments of coast (e.g., at Briatico, Pizzo, Bivona) were flooded and fishing boats were damaged and carried inland. This was also documented at Scalea about 100 km to the

[1]Università di Bologna, Dipartimento di Fisica, settore di Geofisica, Viale Berti Pichat 8, 40127 Bologna, Italy (steve@ibogfs.df.unibo.it, alex@ibogfs.df.unibo.it,)

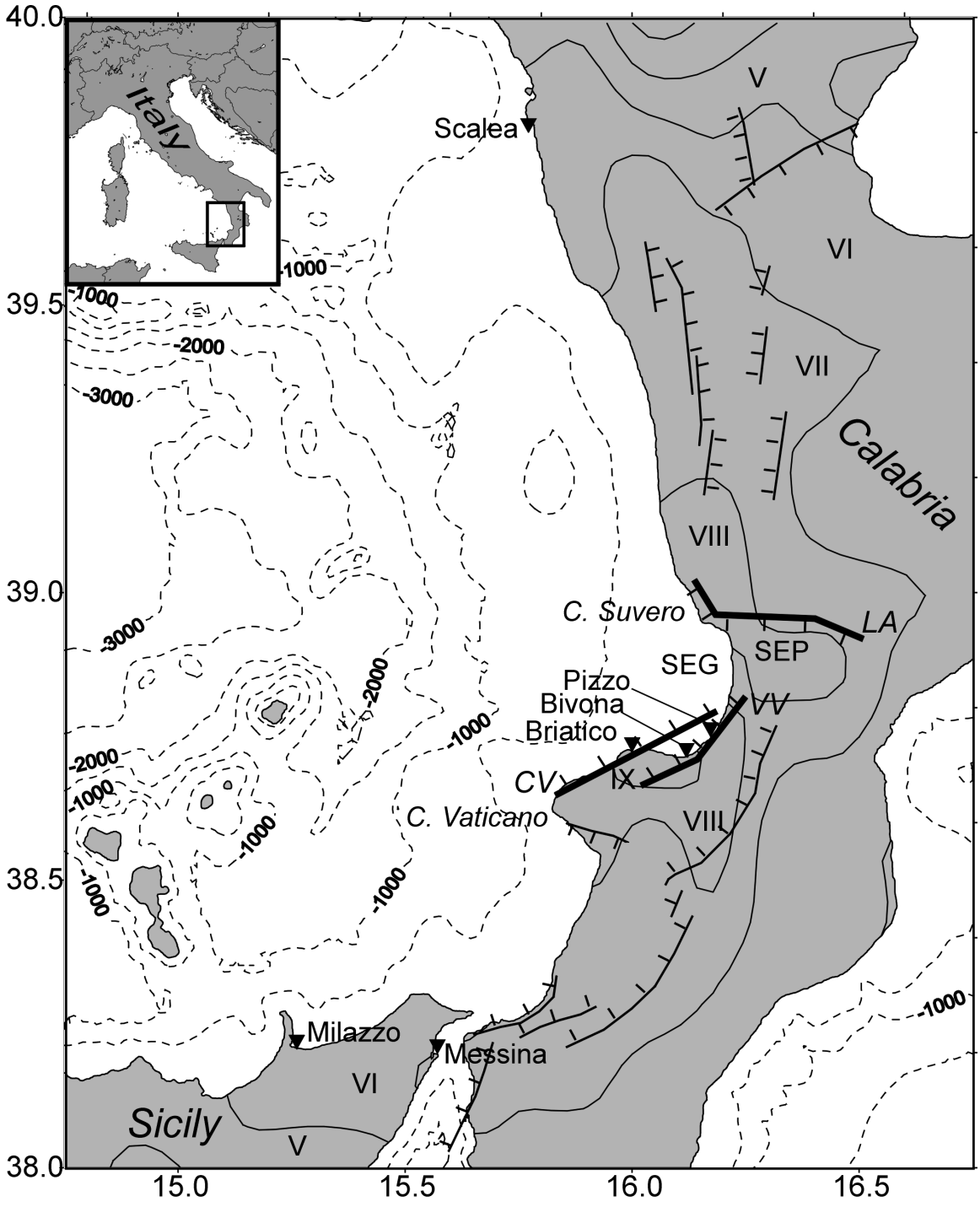

Figure 1: Map of the region involved in the 1905 earthquake and tsunami. Inland solid lines are isoseismals in the MCS scale (data from Boschi *et al.*, 1995). Offshore dashed lines are isobaths (in m). Fault segments from Monaco *et al.* (2000) and Argnani (2000), with hachures denoting the downthrown block. Thick segments are the tsunamigenic sources studied here: (CV) Capo Vaticano, (VV) Vibo Valentia, and (LA) Lamezia faults. SEP: Santa Eufemia Plain, SEG: Santa Eufemia Gulf. Solid triangles are coastal villages where information on tsunami effect is available.

Table 1: Focal parameters of the fault segments used as tsunamigenic sources.

	Strike (deg)	Dip (deg)	Rake (deg)	Slip (m)	Length (km)	Width (km)	Depth of the upper border (km)
CV	245	80	270	2.5	30	20	0.1
VV_1	235	80	270	2.5	15	20	0.1
VV_2	240	80	270	2.5	15	20	0.1
La_1	110	80	270	2.5	10	20	0.1
La_2	90	80	270	2.5	15	20	0.1
La_3	160	80	270	2.5	5	20	0.1

north of the epicenter (see Fig. 1). The tsunami was also observed on the coasts of Sicily. At Milazzo the sea was seen to rise and lower every 30 min with about 80 cm peak-to-peak amplitude. At Messina the tide-gauge was damaged by the earthquake; when some hours later operations started again, oscillations with amplitude of 10 cm and period of 8 min were still persisting. The tsunami was recorded by some tide gauges located in the far field. At Naples and Ischia, some hundreds of kilometers northward and at Civitavecchia, even farther away to the north, tide gauges show first negative arrivals followed by larger positive waves, with peak-to-peak amplitudes between 10 and 18 cm, and periods of about 10–12 min.

2. Source Faults

The main tectonic feature of this region is represented by a segmented normal fault system running along the Apennine chain for a total length of about 180 km (Fig. 1) (Tortorici *et al.*, 1995; Monaco and Tortorici, 2000). Also present are faults striking E–W, namely the Crati Valley and the Lamezia grabens (Argnani, 2000). The focal mechanisms of recent and historical earthquakes show an extensional mode of deformation (Frepoli and Amato, 2000).

The isoseismal map of the 8 September 1905 earthquake (Fig. 1) shows that most damage concentrates along and near the coast (from Capo Vaticano to Capo Suvero) with open isoseismals ideally continuing in the sea, which is suggestive of an epicenter close to the coast. Three active fault segments can be candidates for the source: Capo Vaticano (CV) and Vibo Valentia (VV) faults, both intersecting the epicentral area, and the Lamezia (LA) fault, that is located slightly to the north. All faults are sketched in Fig. 1, and the corresponding focal parameters we used in this work are reported in Table 1: we assume that crustal rigidity is $\mu = 3 \times 10^{10}$ N/m^2, and that each fault is 20 km wide, 30 km long with uniform 2.5 m slip, which corresponds to a seismic moment $M_0 = 4.5 \times 10^{19}$ Nm and a magnitude $M_S \cong 7$, in agreement with the macroseismic magnitude (Boschi *et al.*, 1999). Fault CV separates the Tyrrhenian offshore from the Capo Vaticano peninsula: the foot-wall uplift rate is about 1.5 mm/year (Monaco and Tortorici, 2000).

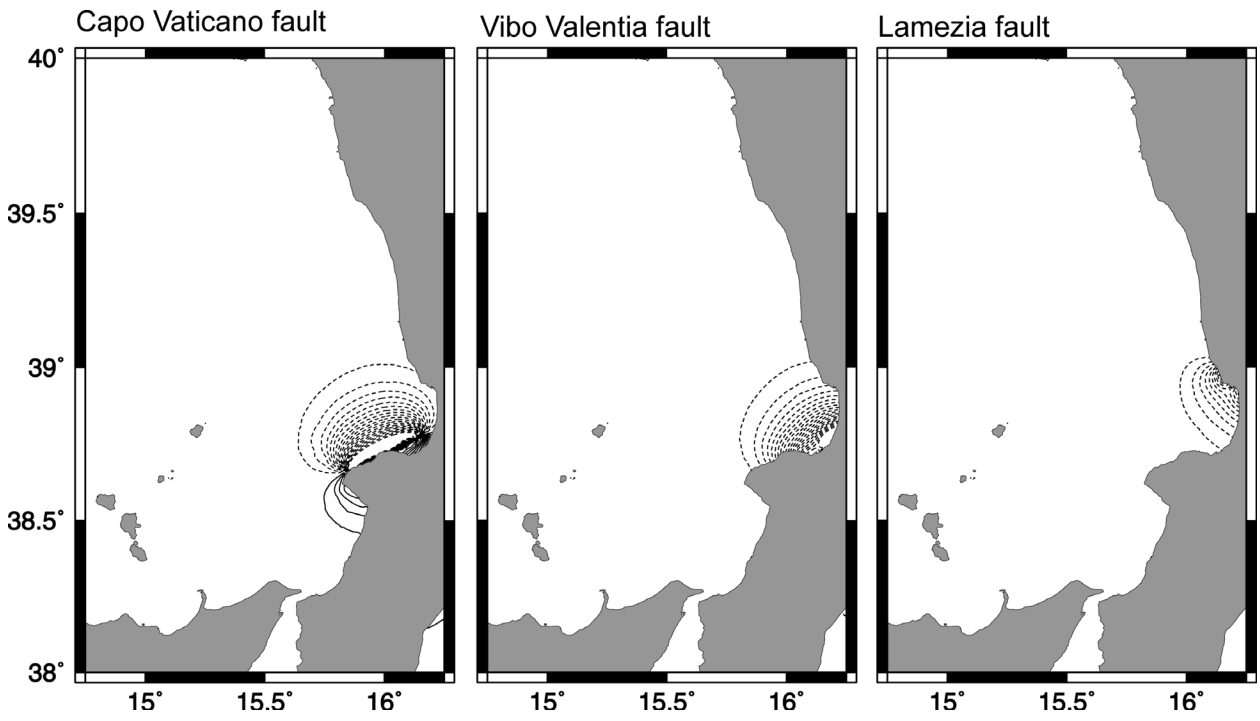

Figure 2: Co-seismic vertical displacement of the sea bottom produced by faults CV, VV, and LA, with parameters listed in Table 1. Contour levels every 5 cm: solid and dashed lines represent, respectively, positive and negative levels.

Here this fault is modeled as a single plane striking 245° and dipping 80°; it produces both co-seismic subsidence and uplifting of the sea bottom (see Fig. 2). Fault VV is formed by two sub-faults, striking 235° and 240°, respectively, with supposedly the same dip as fault CV; it determines a large subsidence of the sea bottom and a minor uplift south of Capo Vaticano. Fault LA consists of three sub-faults striking, from E to W, 110°, 90°, and 160°, with the same dip angle as the above discussed faults. The seafloor displacement is mostly due to the third sub-fault that produces sea bottom subsidence (see Fig. 2).

3. Tsunami Modeling

The tsunami is here modeled as a long wave governed by the equations of the shallow water approximation:

$$\begin{cases} \partial_t \zeta = -\nabla \cdot [(h+\zeta)\mathbf{v}] \\ \partial_t \mathbf{v} = -g\nabla\zeta - \mathbf{v}\cdot\nabla\mathbf{v} \end{cases} \tag{1}$$

In (1) ζ is the water elevation above the mean sea level, h the water depth in a still ocean, $\mathbf{v}$ the depth-averaged horizontal velocity vector, and g the gravity acceleration. The boundary conditions we use for system (1) ensure pure wave reflection on the solid boundary (coastlines) and full wave transmission

on the open boundary (open sea). Equations (1) are solved by means of a finite-element approach (FE), specifically developed for tsunami modeling (Tinti *et al.*, 1994). The initial seawater elevation is assumed to be equal to the co-seismic displacement produced by the fault dislocation, here computed through Okada's analytical model (Okada, 1992), whereas the initial velocity is assumed to be identically null. The computational domain is covered by a FE mesh consisting of 17,296 nodes and 33,278 triangular elements: it includes the source region, the whole Tyrrhenian coast of Calabria, the northeast corner of Sicily, and most of the Aeolian islands. It is large enough to study the near-field features of the tsunami, which is of main interest for this work, but it does not permit the simulation of mareograms of far tide-gauge stations such as Naples, Ischia, and Civitavecchia.

4. Numerical Simulations

We performed numerical simulations of the tsunamis generated by the faults discussed in section 2. The computation time (60 min) is long enough to calculate the main waves in all the most relevant coastal stations. The initial water elevation fields are shown in Fig. 2: the faults onshore (VV and LA) produce a unipolar sea-level displacement (in our case pure subsidence), while fault CV creates bipolar sea-surface displacements. The panels displayed in Fig. 3 refer to the coastal sites given in Fig. 1 and show the calculated tide-gauge records corresponding to the three examined faults: the mareograms are the instantaneous water elevation ζ corrected by the initial elevation ζ_0. In all these localities the sea was seen first to advance and then to retreat, a feature that is not correctly reproduced by fault VV giving oscillations mainly above the old sea level, nor by fault LA, that causes only small fluctuations with opposite polarity of first arrivals. This is poorly satisfied also by fault CV, since it determines a slight inundation followed by a large withdrawal. At Scalea all faults produce a small negative first arrival, followed by a larger positive wave. This is common to all the stations that are outside of the source area (see also the mareograms computed at Milazzo and Messina), and it is noticeably in agreement with the polarity of the first arrivals recorded by the far-field tide gauges of Naples, Ischia, and Civitavecchia.

The maximum water elevation (hereafter MWE) calculated over the entire computation time interval (60 min) along the coastal segments of Calabria and Sicily is shown in Figs. 4a and 4b. The analysis of coastal node elevation within the source region has to account for the co-seismic vertical displacement of the shore. Figure 5, portraying the MWE associated with fault VV along the coast of Calabria, helps us illustrate this point. The solid curve ignores the co-seismic subsidence of the coast due to faulting, and represents the effect of pure hydrodynamic propagation ($\mathrm{MWE}(x,y) = \max[\zeta(x,y,t)]$). On the other hand, the dashed curve is corrected by the initial local elevation ζ_0 and results from the joint action of hydrodynamics and tectonics. In Fig. 4a we plot the MWE along the coast of Calabria, including the ζ_0 correction. It may be observed that the MWE of faults CV

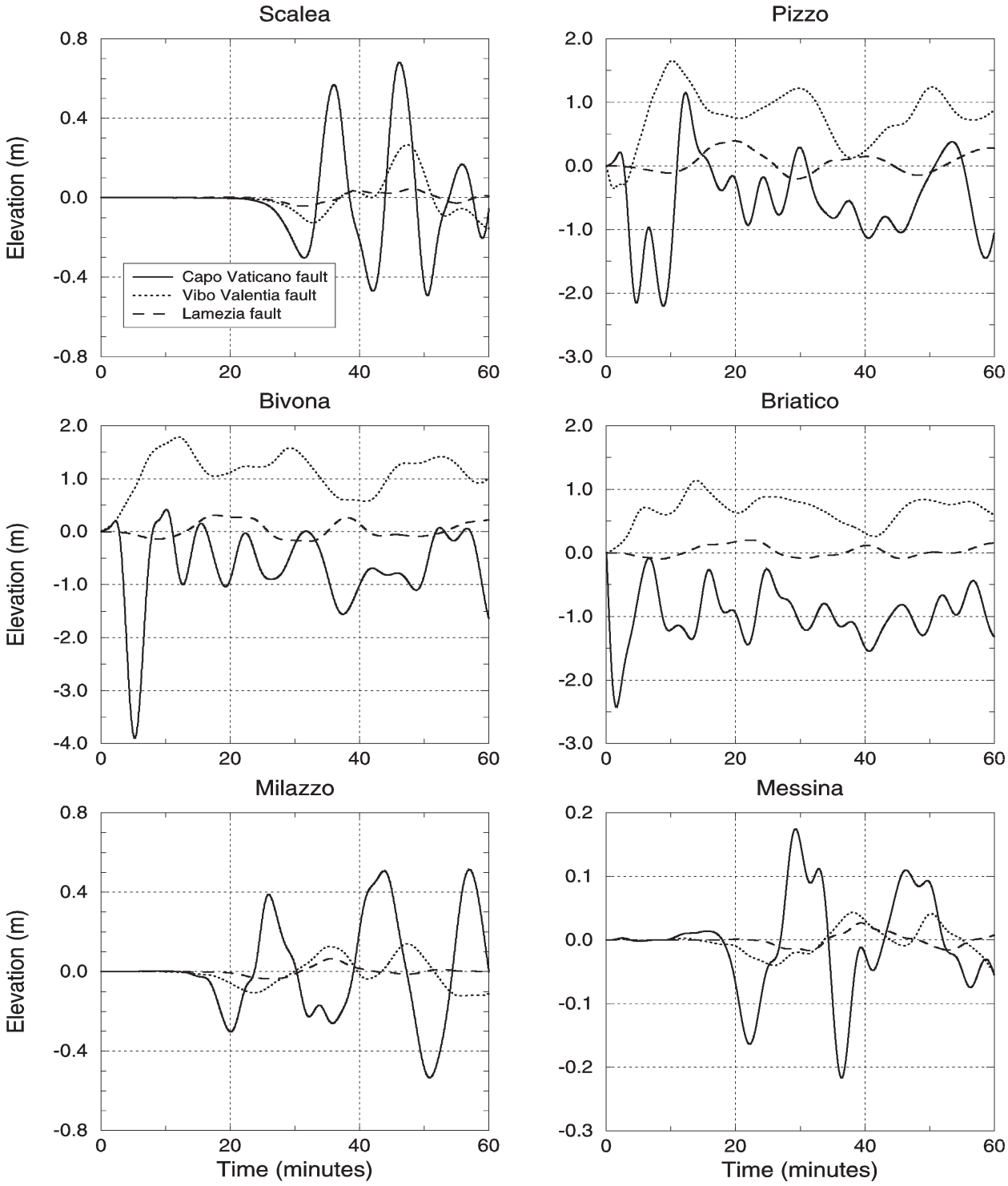

Figure 3: Computed tide-gauge records in the coastal sites shown in Fig. 1. Each panel includes three curves, corresponding to the CV, VV, and LA source faults. Curves start from a zero-level because of the initial-elevation correction.

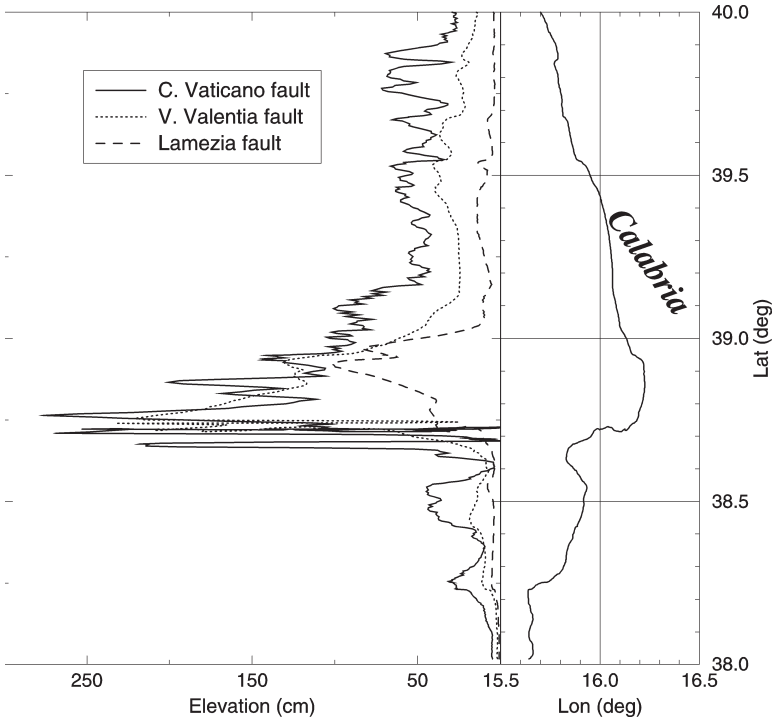

Figure 4a: MWE computed along the coast of Calabria for the three source faults sketched in Fig. 1. It is computed taking into account the co-seismic vertical displacement of the shore due to faulting (see Fig. 2).

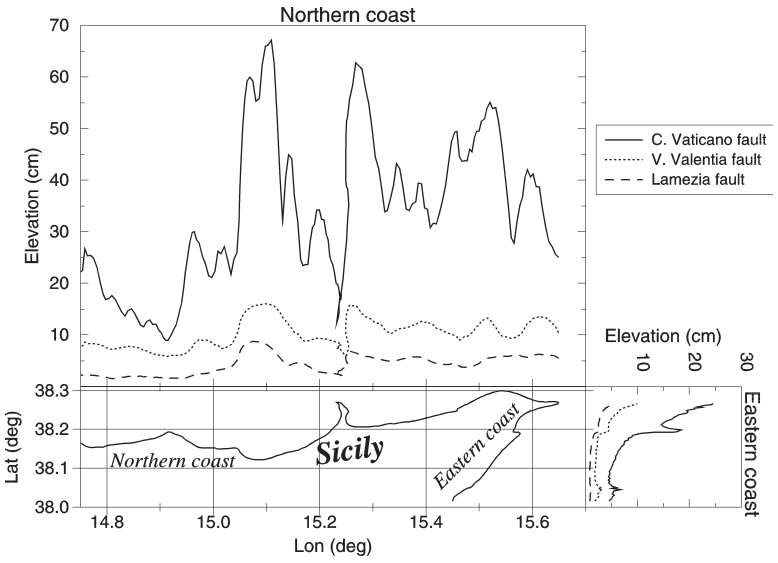

Figure 4b: MWE computed along the coast of Sicily for the three source faults sketched in Fig. 1. It is computed taking into account the co-seismic vertical displacement of the shore due to faulting (see Fig. 2).

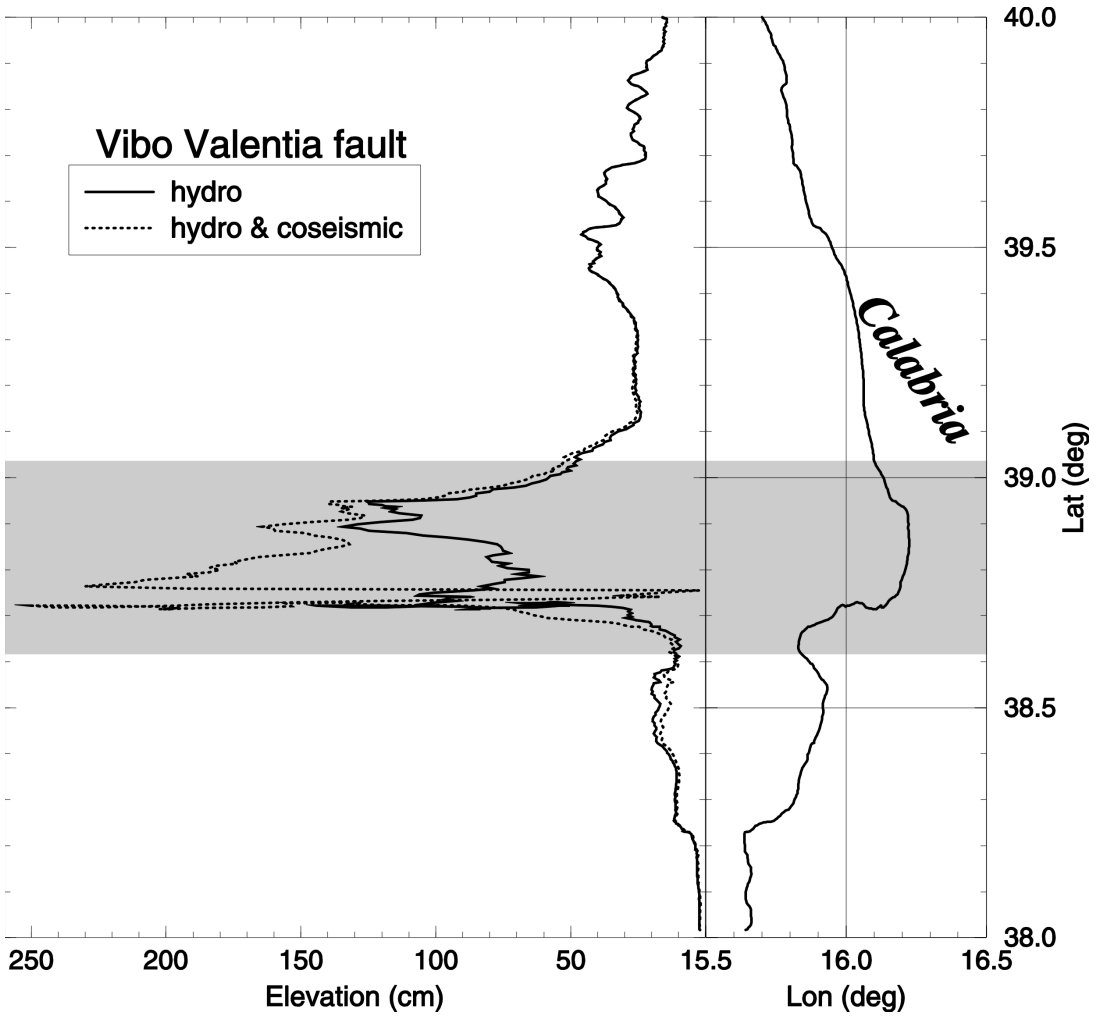

Figure 5: Comparison of the MWE along the coast of Calabria computed by ignoring (solid line) and by taking into account (dashed line) the co-seismic vertical displacement of the shore due to rupturing of the VV fault. The shaded area includes the source region.

and VV are of the same order within the source area, because the co-seismic coastal uplifting produced by fault CV (see Fig. 2) mitigates the effects of the tsunami. Even fault LA produces MWE of the order of 1 m along a short segment belonging to the source region, but MWE is quite small outside this area. The MWEs in Sicily (see Fig. 4b) are relevant only for the tsunami generated by fault CV. In the Messina strait the tsunami effects are negligible, especially for the VV and LA sources.

5. Conclusions

Faults CV, VV, and LA are supposedly normal faults with the same seismic moment. They produce earth-surface displacements that are similar, but they affect very differently the seafloor, owing to the diverse strike and position relative to the coast (see Fig. 2). Therefore tsunami characteristics

are rather different as well. On propagating outside the source, tsunamis keep the hydrodynamic signature of their initial field: the larger the initial perturbation, the larger the tsunami. Therefore, the highest waves are associated with fault CV. However, on the coasts in the near-field wave heights depend also on the tectonic displacement of the shore: coastal subsidence favors flooding, while coastal uplift tends to counteract it. This explains why fault VV and fault CV produce waves of similar penetration and flooding in the coasts of the gulf north of Capo Vaticano (see mareograms of Pizzo, Bivona, and Briatico in Fig. 3): these localities are downlifted and uplifted, respectively, by the former and latter event.

Comparison of the simulation results with the available historical observations do not provide a univocal picture, due also to scarcity of data. The tsunami carried boats inland, flooded low lands in several coastal villages, and produced oscillations in the range of 0.5–1 m in the intermediate field (within the computational mesh: Scalea and Milazzo). The LA earthquake causes a seafloor dislocation too weak and consequently a tsunami too small to be compatible with observations. Which one of the remaining two sources, CV or VV, is to be preferred is not objectively easy to say, since they show both pros and cons. The CV tsunami is more energetic and of comparatively higher frequency than the VV tsunami, hence better explaining the experimental far-field wave heights and periods. However, the VV tsunami better fits the observations in the source region, namely the sea flooding that occurred at Pizzo, Bivona, and Briatico. Our idea is that the agreement with observations can be viewed as satisfactory, and that the parent fault characteristics, namely geometry, position, and source mechanism, cannot be too diverse from the properties of the two sources, CV and VV, that we have considered here. We believe that accordance with observations can be certainly improved by refining the focal parameter values we used in the present simulations.

Acknowledgments. This research was carried out on funds from the Gruppo Nazionale di Difesa dai Terremoti (GNDT) and from the Ministero dell' Università e della Ricerca Scientifica e Tecnologica (MURST).

6. References

Argnani, A. (2000): The southern Tyrrhenian subduction system: Recent evolution and neotectonic implications. *Ann. Geofis., 43*, 585–607.

Baratta, M. (1906): Il grande terremoto calabro dell' 8 settembre 1905. *Atti della Società Toscana di Scienze Naturali, Memorie, 22* (in Italian).

Boschi, E., G. Ferrari, P. Gasperini, E. Guidoboni, G. Smriglio, and G. Valensise (1995): *Catalogo deo forti terremoti in Italia dal 461 a.C. al 1980*. Istituto Nazionale di Geofisica, Roma, Italy (in Italian).

Boschi, E., and Gruppo di Lavoro CPTI (1999): Catalogo parametrico dei terremoti italiani. ING, GNDT, SGA, SSN, Bologna (in Italian), (http://emidius.itim.mi.cnr.it/CPTI/home.html).

Frepoli, A., and A. Amato (2000): Spatial variation in stresses in peninsular Italy and Sicily from background seismicity. *Tectonophysics, 317*, 109–124

Monaco, C., and L. Tortorici (2000): Active faulting in the Calabrian arc and eastern Sicily. *J. Geodynamics, 29*, 407–424.

Okada, Y. (1992): Internal deformation due to shear and tensile faults in a half-space. *Bull. Seismol. Soc. Am., 82*, 1018–1040.

Piatanesi, A., and S. Tinti (1998): A revision of the 1693 eastern Sicily earthquake and tsunami. *J. Geophys. Res., 103*, 2749–2758.

Piatanesi, A., S. Tinti, and E. Bortolucci (1999): Finite-element simulations of the 28 December 1908 Messina Straits (southern Italy) tsunami. *J. Phys. Chem. Earth, 24*, 145–150.

Platania, G. (1907): I fenomeni in mare durante il terremoto di Calabria del 1905. *Boll. Soc. Sism. Ital., 12*, 43–81 (in Italian).

Tinti, S., and A. Maramai (1996): Catalogue of tsunamis generated in Italy and in Côte d'Azur, France: A step toward a unified catalogue of tsunami in Europe. *Ann. Geofis., 39*, 1253–1299 (corrections in *Ann. Geofis., 40*, 781, 1997).

Tinti, S., and A. Piatanesi (1996): Finite-element simulations of the 5 February 1783 Calabrian tsunami. *J. Phys. Chem. Earth, 12*, 39–43.

Tinti, S., I. Gavagni, and A. Piatanesi (1994): A finite-element numerical approach for modeling tsunamis. *Ann. Geofis., 37*, 1009–1026.

Tinti, S., A. Armigliato, E. Bortolucci, and A. Piatanesi (1999): Identification of the source fault of the 1908 Messina earthquake through tsunami modeling. Is it a possible task? *J. Phys. Chem. Earth, 24*(B), 417–421.

Tinti, S., A. Armigliato, and E. Bartolucci (2001): Contribution of tsunami data analysis to constrain the seismic source: The case of the 1693 eastern Sicily earthquake. *J. Seismol., 51*(1), 41–61.

Tortorici, L., C. Monaco, C. Tansi, and O. Cocina (1995): Recent and active tectonics in the Calabrian arc (Southern Italy). *Tectonophysics, 243*, 37–55.